Grain boundary diffusion of titanium in polycrystalline quartz and its implications for titanium in quartz (TitaniQ)

Grain boundary diffusion of titanium in polycrystalline quartz and its implications for titanium in quartz (TitaniQ) geothermobarometry.

Geoffrey David Bromiley[1*] and Matthew Hiscock[1,2]

1. School of GeoSciences and Centre for Science at Extreme Conditions, King's Buildings, University of Edinburgh, Edinburgh, EH9 3FE UK.
2. Oxford Instruments NanoAnalysis, Halifax Road, High Wycombe, HP12 3SEUK.

*corresponding author:
Email: geoffrey.bromiley@ed.ac.uk
Tel: +44 (0)1316508519 or +44(0)7913626360
Fax: +44 (0)1316507340

Abstract

We have performed a series of experiments to measure diffusivity of Ti in polycrystalline quartz under high pressure/temperature, nominally anhydrous conditions. Resulting diffusion profiles reveal operation of both slow lattice diffusion and faster grain boundary diffusion. Over the temperature range investigated, 1000-1400°C, grain boundary diffusion of Ti is between 3 and 4 orders of magnitude faster than lattice diffusion and can be expressed by the following Arrhenius relationship:

$$D(m^2/s) = 2.00 \pm 0.08 \times 10^{7} \exp(-195 \pm 7\ kJ.mol^{-1}/RT)$$

Grain boundary diffusion is expected to have a considerable influence on Ti mobility in the crust in Si-rich rocks under fluid-absent conditions, especially in fine-grained rocks, with grain boundaries acting as fast conduits for transporting Ti. This has important consequences for the application of Ti in quartz geothermobarometry (TitaniQ). Grain boundary diffusion is a viable mechanism for re-equilibrating Ti contents in quartz-rich rocks to lower values, for example during dynamic recrystallization. This implies that TitaniQ can

be applied to relatively low temperatures (below 600°C) although zonation of Ti contents in larger quartz grains is expected due to the relative sluggishness of lattice diffusion under these conditions and because fast diffusion in grain boundary regions effectively inhibits growth entrapment. Grain boundary diffusion for Ti also has implications for the activity of Ti in quartz-rich rocks and application of the TitaniQ geothermobarometer.

Key words: quartz, TitaniQ, diffusion, grain-boundaries

1. Introduction

Geological thermometers and barometers provide key information needed to constrain the crystallization history of igneous and metamorphic rocks, providing valuable insight into geological processes powering their formation. Since its initial calibration by Wark and Watson (2006) the Ti-in-quartz (or TitaniQ) geothermobarometer has been applied to a wide variety of rocks in variable geological settings. This technique relies simply on the dependence of concentration of Ti in quartz $[Ti]_q$ with temperature, with a correction for Ti activity in cases where systems are Ti undersaturated. More recently, the coupled pressure and temperature dependence of $[Ti]_q$ has been determined to allow the TitaniQ technique to be used to determine pressure and/or temperature in silica-rich rocks (Huang and Audetat, 2012; Thomas et al., 2010, 2015). The TitaniQ technique has several important advantages over other commonly used thermobarometers in that: 1) unlike many other methods it can be readily applied to felsic rocks, 2) it is not easily reset in altered or weathered rocks, and 3) it is not reliant on complex element partitioning between multiple phases (not withstanding issues over Ti activity). Analysis of $[Ti]_q$ by electron microprobe (EMP) allows easy and routine application of TitaniQ for crystallization temperatures exceeding 600°C. Secondary Ion Mass Spectrometery allows this range of temperatures to be extended, in theory, as low as 400°C. Consequently, applications of this method have been diverse, including determining temperature estimates in: 1) high grade metamorphic rocks (e.g. Ashley et al., 2013; Sato and Santosh, 2007; Spear and Wark, 2009), 2) hydrothermal veins (e.g. Ashley

et al., 2013; Barker et al., 2010; Müller et al., 2010; Rusk et al., 2008; Sato and Santosh, 2007; Spear and Wark, 2009), 3) magmatic rocks and migmatites (e.g. Cole et al., 2014; Girard and Stix, 2010; Storm and Spear, 2009; Vazquez et al., 2009; Wark et al., 2007), and 4) to mylonites and deformed rocks (e.g. Grujic et al., 2011; Kohn and Northrup, 2009; Pennacchioni et al., 2010).

Application of TitaniQ, especially towards lower temperatures where element mobility is inherently more sluggish, requires an efficient mechanism for re-equilibrating $[Ti]_q$. Published data on Ti diffusion in single crystal quartz (Cherniak et al., 2007) indicate, as expected, that lattice diffusion is too slow to allow effective equilibration of [Ti] over geological relevant timescales except at relatively high temperatures. Instead, it is typically assumed that melts or fluids play a key role in transporting Ti. In magmatic systems or in hydrothermal veins or bodies this is an obvious assumption to make. However, application of TitaniQ in other settings requires some validification of Ti transport mechanisms. In polycrystalline material grain boundaries can act as conduits for fluid flow which may greatly enhance Ti mobility, and previous studies have hypothesized the role that fluids may have in both driving grain boundary migration and in enhancing Ti lattice diffusion (e.g. Bestmann and Pennacchioni, 2015). The presence of a grain boundary fluid might be expected to result in clear textural evidence, such as fluid inclusions; the absence of such evidence means that application of TitaniQ must be treated with caution. However, even in the absence of fully permeating fluids, grain boundaries can still act as fast pathways for element transport. The importance of (fluid-absent) grain boundary diffusion in polycrystalline aggregates is well known in the fields of solid-state chemistry and materials science (see Sutton and Balluffi, 1995, Mehrer, 2007, and Dohmen and Milke, 2010 for a general review). However, to date, experimental and analytical challenges mean that experimental studies of grain boundary diffusion under high-pressure/temperature conditions in geologically relevant systems are limited (e.g. Demouchy, 2010a, b; Hayden and Watson, 2008). Here, we present the first experimental data on Ti grain boundary diffusion in polycrystalline quartz under (fluid-absent) high-

85 pressure conditions of the lower crust. Results allow us, in combination with the data of
86 Cherniak et al. (2007), to assess the mobility of Ti in quartz-rich rocks within the crust and
87 the applicability of the TitanQ technique towards lower temperatures in melt- and fluid free
88 (or poor) systems.
89
90 **2. Experimental procedure**
91 Experiments were performed using a source-sink design which promotes Ti diffusion from a
92 Ti capsule (source) into and through a matrix of synthetic, fine-grained polycrystalline quartz
93 (sink). 5mm long, 4mm o.d., 0.3mm wall thickness capsules with hammer fit lids were
94 machined from high purity (99.999%) Ti rod. Capsules are similar to those described in
95 Bromiley et al. (2004), and are designed to seal effectively during loading to prevent volatile
96 exchange into or out of the sample during high-pressure/temperature experiments. These
97 thick-walled capsules also minimize deformation of the capsule interior (Ayers et al. 1992).
98 Capsules were first annealed in air to promote oxidation of surface layers to TiO_2. SEM
99 imaging of run products revealed that this produced a 20 micron thick oxide layer. High-
100 purity quartz was used for diffusion experiments, which had been pre-synthesized under
101 anhydrous conditions at 300 MPa, 900°C from 99.995% SiO_2. Due to variable grain growth
102 during annealing, synthesised quartz was crushed and sifted to a grain size of ~10-30μm to
103 ensure an even, small grain size during diffusion experiments. Quartz was stored at 130°C
104 to drive off any volatiles before being loaded into capsules. In selected runs, 10μl of
105 deionized water was also added during loading to achieve water-saturated conditions in
106 quartz during diffusion experiments. High-pressure/temperature (HPT) experiments were
107 performed using an end-loaded piston-cylinder apparatus with 0.5” talc-pyrex-graphite
108 assemblies, as described in more detail in Bromiley et al. (2010). No additional pressure
109 calibration of the capsule design used here was conducted, although Ayers (1992) note that
110 thick walled transition metal capsules (including Ti) have no effect on pressure loss due to
111 friction in piston-cylinder assemblies. Temperature was measured using a Pt-Pt13%Rh
112 thermocouple placed close to the top of the capsule. Runs were pressurized using the hot-

piston out technique, pressure and temperature continually monitored and maintained throughout, and quenched rapidly (<10s) by turning off power to the heating circuit. Presence of water in recovered hydrous experiments was determined by carefully weighing capsules before and after experiments. Recovered capsules were prepared as a series of discs cut perpendicular to the long axis of the capsule which were then mounted in epoxy and polished using SiC and diamond pastes prior to analysis.

3. Sample examination and analysis

Recovered, sectioned capsules were first examined optically and by scanning electron microscope (SEM). Ti contents of quartz grains within the capsule were determined using a Cameca SX100 electron microprobe equipped with 5 spectrometers. Initially, sectioned capsules were examined by EMP to verify that Ti diffusion had occurred and examine relationships between the capsule, oxide layer and experimental charge. In later analyses used for fitting diffusion laws, Ti capsules were carefully removed from the run products prior to EMP analysis. Analysis was performed using a 20kV accelerating voltage and 60 nA beam current, resulting in a beam size of approximately 2 μm diameter. Ti Kα X-rays were simultaneously counted on PET crystals (3 overlarge, one standard size) in four spectrometers and standardized to synthetic rutile using a method similar to that outlined in Wark and Watson (2006), yielding a detection limit of ~5 ppm. Si Kβ X-rays were also counted on one TAP crystal to verify that analyzed crystals were SiO_2. Point analyses were made in regions of quartz grains as close to grain boundaries as possible, in order to minimize the effects of lattice diffusion of Ti through quartz. Numerous diffusion profiles across different transects were obtained from each recovered sample. Consistency in data obtained across different transects meant that data could be readily amalgamated to produce averaged diffusion profiles for each sample. Parameters discussed below were obtained by fitting diffusion laws to these averaged diffusion profiles. Fitting diffusion laws to individual diffusion profiles produced, within error, similar results. After EMP analysis,

polished sections were re-analyzed by SEM so that distance of analysis points from the edge of the sample (TiO_2 boundary layer) could be determined as accurately as possible, and to verify that all analysis points were from central regions of crack and inclusion-free quartz crystals.

4. Results and data fitting

Experimental conditions used in successful experiments are listed in Table 1. A typical diffusion profile is shown in Figure 1a. The experimental design used promotes diffusion of Ti from the capsule wall into the sample of polycrystalline quartz. For a simple case where we consider that Ti diffuses through the polycrystalline quartz by a simple, single mechanism, i.e. lattice diffusion, data can be fitted to a standard solution of Fick's 2nd law. Here we assume that the capsule acts as a constant Ti source, with Ti diffusing into a semi-infinite sink, such that:

$$C(x,t) = (1 - erf\frac{(x-x_0)}{2\sqrt{D_{eff}t}}) * C_0 \qquad [1]$$

where $C(x,t)$ is the concentration of the diffusant (Ti) at distance x from the source (i.e. capsule wall at distance x_0) after time t, D_{eff} is the effective diffusion coefficient, and C_0 is the concentration of the diffusant in the sink at t=0 (confirmed by EMP analysis to be below the detection limit and assumed to be zero). The dashed line in Figure 1a shows a fit of this solution to the typical diffusion profile. In all cases it is evident that data cannot be adequately fitted to a single diffusion law, implying that a single diffusion mechanism cannot fully explain Ti mobility during the experiments. In all cases it is also evident that diffusivity of Ti is at least an order of magnitude faster than would be expected based on LD of Ti in quartz (Table 1). For comparison, data from Cherniak et al. (2007) suggests that under conditions of experiment TiQ9 which produced the diffusion profile shown in Figure 1a, lattice diffusion would only account for Ti migration of up to a few microns into the sample.

From the absence of a fluid or melt phase in the experimental charges it is clear that grain boundary diffusion plays an important contribution to Ti mobility in polycrystalline quartz, and that experiments represent a type B kinetic regime of (Harrison, 1961). Accordingly, we note that in accordance with type B kinetics, the following relation holds in all experiments:

$$\delta << (D_{eff}t)^{0.5} << \Phi/2 \quad [2]$$

using measured grain size, Φ, and making a reasonable assumption for grain boundary width, δ, of the order of $1x10^{9}$ m.

In order to separate the effects of lattice and grain boundary diffusion, and to determine the grain boundary diffusion coefficient, D_{gb}, we used the relationship of Leclaire (1963) as derived from the constant source solution of Whipple (1954), such that:

$$s\delta D_{gb} = q.\sqrt{\frac{D_L}{t}}.\left[\frac{\partial ln\bar{C}_{ave}(x,t)}{\partial\left(x^{\frac{6}{5}}\right)}\right]^{\frac{-2}{p}} \quad [3]$$

where s is the segregation factor (between quartz grains and grain boundaries), δ is the grain boundary width, C_{ave} is the average concentration of the diffusant at distance x from the source, and p=6/5 and q=1.322. The product $s\delta D_{gb}$ can be solved graphically by plotting lnC_{ave} vs $x^{6/5}$, as shown in Figure 1b. In this plot, the initial steep part of the diffusion profile can be assigned to LD of Ti into quartz grains, with the subsequent straight line region assigned to grain boundary diffusion. As data were obtained within quartz grains but adjacent to grain boundaries, Ti concentrations effectively represent averaged values at distance x from the Ti source, and diffusion profiles are not additionally overprinted by the effects of varying degrees of lattice diffusion within quartz grains at a given distance x. Typically, an insufficient number of data points were available to meaningfully fit the first part

of diffusion profiles to LD, so we instead used data from Cherniak et al. (2007) to model data and obtain D_{gb}. In accordance with numerous previous studies we assumed a lower estimate of grain boundary width of 0.75 nm (e.g. Demouchy, 2010a, b), and assume a segregation factor of 1. Results of fitting are listed in Table 1.

5. Discussion

5.1 Sample characterization and diffusion mechanism

Ti capsules in this study act as the source of Ti diffusing into the polycrystalline quartz. In nature, Ti is incorporated in minerals dominantly as Ti^{4+}, and only rarely as Ti^{3+}, for example under the very reducing conditions of the lunar interior. However, the fact that Ti is a multivalent element, and that experiments described here are nominally unbuffered with respect to oxygen, necessitates careful consideration of Ti speciation in the present study. Oxidation of Ti capsules to TiO_2 would impart extremely reducing conditions on the sample assembly, sufficient in fact to reduce SiO_2 to Si metal. Examination of run products demonstrates that this is clearly not the case; both high magnification optical and SEM imaging of run products exclude growth of oxide rims, coloration due to the presence of reduced Ti oxides, or reduction of silica. This is consistent with the common observation that Ti remains inert even up to high temperatures due to the stability of thin TiO_2 films. Ti has been used successfully as an encapsulating metal in many high-pressure experiments (as initially described in Ayers et al., 1991), and Wu and Koga (2013) have demonstrated that transition metal capsules are actually ineffective at influencing fO_2 conditions in sample assemblies. We observed this directly in trial experiments. During volatile-free runs using thick-walled Ti capsules with additional synthetic TiO_2 oxide layers interspersed throughout polycrystalline quartz, we observed that recrystallized rutile crystals in recovered run products were colourless to light blue. This indicates the presence of only trace amounts of Ti^{3+}, indicating that Ti was dominantly Ti^{4+}; this is in marked contrast to the intense dark blue colour noted in H-saturated rutile which has been reduced (e.g. Bromiley and Hilairet, 2005; Bromiley and Shiryaev 2006). This indicates that although unbuffered, fO_2 conditions within

Ti capsules cannot be significantly different from those encountered in nature, and that importantly, Ti within samples is dominantly stable as Ti^{4+}.

EMP examination of polycrystalline quartz indicates clear Ti diffusion profiles from the capsule wall/quartz interface into the center of the sample volume. Ti is typically incorporated into the quartz structure as Ti^{4+} (e.g. Ashley et al., 2013;Thomas et al., 2010), although Ti can also be incorporated into quartz in lower oxidation states such as Ti^{3+}, typically coupled with other defects such as Fe^{3+} (e.g. Cohen and Makar 1985). The analytical approach used here to fit data distinguishes between lattice diffusion in quartz and the the dominant transport process, grain boundary diffusion. As such, although analysis of run products or comparison with data in the literature might be used to indicate Ti incorporation mechanisms within quartz grains, they would not indicate Ti speciation and Ti incoporation in grain boundary regions. As such, speciation of Ti in quartz grain boundary regions, and Ti transport mechanisms can only be inferred from circumstantial evidence. Ti capsules used in this study contain thin TiO_2 oxide layers. Importantly, we do not observe any growth in oxide layers in recovered run products. Given that in the absence of other species such as Fe^{3+}, Ti is favourably incorporated into quartz as Ti^{4+} substituting directly for Si^{4+}, it is likely that the dominant transport process occuring in experiments is direct Ti-Si exchange and Ti^{4+} migration; namely, that Ti is incorporated into, and mobile within grain boundary regions as Ti^{4+}. Coupled with Ti diffusion into quartz, during initial analysis of run products we also observed Si incorporation into the oxide layer of Ti capsules. EMP analysis of oxide rims of the Ti capsules revealed the presence of <1 weight % silica. In contrast, Ti capsules remained Si-free (at the detection limit of Si of a few hundred ppm). This is consistent with direct Si^{4+} - Ti^{4+} exchange between the capsule rims and quartz, but not with Si-Ti oxidation/reduction which would be required for Si diffusion into Ti metal.

In contrast, diffusion of species such as Ti^{3+} or Ti^{2+} would require some additional charge balancing mechanism. Use of synthetic, spec pure silica essentially prevents coupled

diffusion of defects other than Si, Ti and O. H^+ incorporation into quartz could charge-balance Ti^{3+} incorporation, for example via a coupled mechanism of Ti^{3+} + H^+ diffusion into the experimental charge. However, for the experimental durations used, use of anhydrous starting materials and thick-walled Ti capsules effectively inhibit H incorporation in the sample. Furthermore, examination of run products by IR spectroscopy failed to reveal the presence of characteristic O-H stretching bands in quartz which should be very readily detectable. Ti^{3+} diffusion could be charge balanced alternatively by coupled diffusion of oxygen vacancies. This would then require net flux of oxygen out of the sample volume. Ti capsules remain effectively sealed during experiments, implying that diffusing oxygen could not be readily lost from the capsule. We observed no evidence for further oxidation of Ti capsules which could act as a sink for this oxygen, although growth of oxide layers via such a mechanism could conceivably be too small to be easily observed. Flux of oxygen towards the TiO_2 oxide layer would, however, result in an effective increase in fO_2 near the edge of the sample. This would then be inconsistent with continued Ti^{4+} reduction in the oxide layer and diffusion of Ti^{3+} during diffusion experiments. As such, it is difficult to justify coupled Ti^{3+}-oxyygen vacancy diffusion as an important mechanism throughout the duration of experiments performed here.

Alternatively, Ti^{3+} diffusion through quartz grain boundaries could take place by a coupled mechanism involving coupled incorporation and 'hopping' of Ti^{3+} onto/across both Si^{4+} sites and interstitial Ti^{3+}. Such a mechanism would require reduction of Ti^{4+} at the oxide layer, and is, of course, inconsistent with the observed diffusion of Si into the oxide layer or inferred fO_2 conditions. However, flux of some Ti in grain boundary regions of quartz as Ti^{3+} cannot be discounted, either here or in nature, where Ti^{3+} defects in quartz are commonly observed in small quantities coupled to other subsitutional defects. However, on balance, observations indicate that Ti^{4+}-Si^{4+} exchange between quartz and the oxide layer is the dominant process occuring during the experiments. Clearly, further investigation of element speciation in grain boundary regions is required, although this remains analytically extremely challenging.

In contrast to anhydrous experiments, H-present diffusion experiments were unsuccessful due to a number of experimental difficulties. Some higher temperature experiments (>1000°C) suffered from water-loss (as detected by weight loss) presumably due to failure of the Ti capsule. Presence of an unknown Ti-Si-rich hydrous phase in grain boundary regions within the polycrystalline matrix was also noted in recovered samples from successful experiments. The texture of this phase indicates that it is probably a quenched (hydrous) melt. In experiment TiQ11 Ti diffusion profiles within the polycrystalline quartz could be measured, and the melt phase was confined to regions of the sample immediately adjacent to the capsule wall. As such, diffusion profiles could be obtained from regions of the same which were melt-free. However, uncertainties in how diffusion data from such experiments can be interpreted, and observed grain growth in H-present experiments means that results cannot be meaningfully used.

5.2 Temperature dependence of Ti diffusivity

Figure 2 is an Arrhenius plot showing the temperature dependence of D_{gb}. Over the temperature range investigated, 1000-1400°C, grain boundary diffusion of Ti in quartz is between 3 and 4 orders of magnitude faster than LD of Ti^{4+}, as constrained by Cherniak et al. (2007). Calculated activation energy from the Arrhenius plot in Figure 2 is 195±7 kJ/mol, in comparison to 273±12 kJ/mol for lattice diffusion of Ti in quartz from Cherniak et al. (2007). Lower activation energy associated with grain boundary diffusion is consistent with a generally lower free energy barrier for Ti migration between defect sites in grain boundary regions. This is in general agreement with results of molecular dynamic simulations of near-surface environments in quartz by Lanzillo et al. (2014), who calculated substantially lower free energy barriers for Ti diffusion close to oxygen-terminated quartz surfaces. However, Lanzillo et al. (2014) predicted a cross-over in log diffusivity of near-surface (i.e. grain boundary) vs lattice diffusion of Ti in quartz at high T (their figure 7b) which we do not note, and predicted a difference in E_A a factor of 2-3 lower, which is substantially higher than we

observe. Broadly similar temperature dependences for grain boundary and lattice diffusion as noted here have, however, also been observed in other studies of polycrystalline materials (e.g. Nogueira et al., 2003).

From experiment TiQ11 it is clear that Ti diffusivity is significantly enhanced. In regions adjacent to capsule walls this could be due to the presence of a hydrous melt phase. However diffusion profiles consistent with enhanced Ti diffusivity extend into the experimental charge into regions in which additional phases at grain boundaries are not observed. However, as grain growth had occurred in the quartz, which might have acted as an additional mechanism to modify Ti contents of quartz grains, and as we cannot readily ascertain whether a free fluid phase was present throughout the sample, we cannot readily draw meaningful interpretation of the results.

5.2 Importance of grain boundary diffusion on Ti mobility and geothermobarometry

Assuming that the width of grain boundaries in polycrystalline quartz is approximately constant (i.e. of the order of 1 nm), the relative importance of grain boundary diffusion vs lattice diffusion of Ti in fluid- and melt-free quartz-rich rocks will depend on grain size and temperature. Assuming a segregation factor of s=1, a lower estimate of grain boundary width of 0.75 nm and using equation 3, with D_{gb} from Table 1 and D_L from Cherniak et al, (2007), we have calculated effective total diffusion of Ti in polycrystalline quartz, D_{eff}, for a range of grain sizes for each data point in Figure 2. Results are shown in the Arrhenius plot in Figure 3. Extrapolation to lower temperatures highlights the key role which grain boundary diffusion plays in mobilizing Ti in fine-grained quartz under conditions of the lower crust, with a 6 order of magnitude difference in flux of Ti in 1cm compared to 1μm polycrystalline quartz at 600°C. Even in the absence of a fluid phase it is clear that grain boundaries act as important conduits for mobilizing Ti in quartz-rich rocks. To highlight this, we have also calculated the temperature dependence of characteristic diffusion distance for this range of quartz grain sizes for 2 geologically relevant end-member scenarios: (1) t=10^5 years, as a model of small-

scale thermal perturbations in the crust such as those related to a large igneous intrusion, and (2) t=10^7 years, as a model of thermal perturbations in the crust related to large-scale tectonic activity. Results, shown in Figure 4, can be used to assess the mobility of Ti in different model scenarios and to consider the ease with which the TitaniQ geothermobarometer can be reset in systems in which an abundant melt or fluid phase is either absent or cannot be proven. This is particularly relevant to the use of the TitaniQ method at lower temperatures in metamorphic terrains and areas of dynamic recrystallization. For fine-grained quartz-rich rocks (grain sizes of approximately 10 μm), and relatively short period of 10^5 years, Ti is mobilized over a limited distance of the order of cms at the lowest temperatures to which the TitaniQ thermobarometer is applied (500-800°C). Over a period of 10^7 years, however, mobilization of Ti is more extensive, of the order of several 10s of cms. Even in coarser grained rocks (100 μm grain size), Ti is mobilized on this time scale over distances of cm to 10s of cm. Figure 4 clearly demonstrates that in regional metamorphic settings, resetting of the TitaniQ thermobarometer is expected in finer grain rocks.

For calculations described here, in the absence of any direct determination of partitioning of Ti between quartz crystals and grain boundary regions, we assume a segregation factor of unity. Trace element concentrations in grain boundary regions cannot readily be measured due to spatial limitations in analytical techniques, so the actual segregation factor of Ti in quartz is not easily determined. It is, however, generally assumed that higher point defect and vacancy concentrations in grain boundary regions could result in higher solubilites of incompatible elements, and there is some limited data which indicates that this might be the case, at least for highly incompatible elements in mantle rocks (Hiraga et al. 2003, 2004). To explore the effects of segregation of Ti into grain boundaries, we recalculated characteristic diffusion distances using a high segregation factor, s=20. This segregation factor is based on the assumption that Ti solubility in quartz grain boundary regions is the same as Ti solubility in a siliceous melt of the same composition, using data from Hayden and Watson

(2007). This is obviously a flawed assumption, as grain boundary regions are far from being amorphous, although it does provide a useful end-member scenario for investigating the full effects of large degrees of grain boundary segregation of Ti. Dashed lines in Figure 4 show corresponding characteristic diffusion distances for the 5 different modelled grain sizes using this end-member high segregation factor. Characteristic diffusion distances are significantly reduced, especially in finer-grained aggregates. This implies, in cases of significant grain-boundary/crystal fractionation, that only very localized remobilization of Ti can occur in fine-grained quartzite over periods of 10^5 years. However, even with significant fractionation, cm scale remobilization of Ti occurs over long timescales of 10^7 years, even in coarser grain quartzite (100 μm grain size). Clearly, accurate determination of segregation factors is required in order to fully determine the geological importance of grain boundary diffusion, and in particular, to correctly determine grain boundary diffusivities from experimental studies. Furthermore, additional factors such as variations in grain boundary width in different systems clearly require investigation. However, even cursory examination of run products from the present study demonstrates that Ti mobility in fine-grained (10-30 μm) quartz aggregates is very significantly enhanced relative to Ti mobility in single crystal quartz, and modelling of data, even assuming very high segregation factors for Ti, validates the importance of grain boundary diffusion as a mechanism for mobilizing Ti.

Recently, there have been several attempts to apply the TitaniQ thermobarometer to mylonites and other deformed metamorphic rocks, and ongoing controversy over the scientific justification of applying the technique at low temperatures in deformed quartz. It is commonly assumed that incorporation of incompatible trace elements into mineral structures can be predicted by considering resulting lattice strain of the host structure, such as in the well-known model of Blundy and Wood (2003). Recent high-precision X-ray diffraction data (Ashley et al., 2013), X-ray absorption studies and molecular dynamics simulations (Thomas et al., 2010) support the supposition that Ti^{4+} substitutes directly for Si^{4+} and is incorporated onto tetrahedral sites in the quartz structure. The substantial size mismatch between Ti^{4+}

and Si^{4+} would, therefore, be expected to result in considerable lattice strain in quartz. Although the relationship between lattice strain arising from Ti substitution and Ti concentration in quartz will be non-linear due to effects such as clustering of Ti defects at high concentrations, this obvious size mismatch explains the strong temperature dependence which is the basis of the TitaniQ geothermobarometer. The extent to which a technique such as TitaniQ can be applied in low temperature deformed terrains depends on the efficiency of Ti mobility at low temperatures and the possible additional effects of deformation (i.e. additional lattice strain) on mineral chemistry. The extent to which deformation might influence $[Ti]_Q$ has been the subject of several recent investigations. Atomistic simulations of Ashley et al. (2013) indicated that resetting $[Ti]_Q$ during dynamic recrystallization can only occur to a limited extent due to processes such as sub-grain rotation and migration of dislocation arrays. In high-strain deformation experiments using single crystal, fluid-bearing quartz, Negrini et al. (2014) found abundant evidence for recrystallization processes such as grain boundary migration recrystallization and sub-grain rotation, but noted that these did not result in re-equilibration $[Ti]_Q$ in experimental charges. In contrast, in a systematic investigation of dynamically recrystallized quartz Bestmann and Pennacchioni (2015) found strong evidence of re-equilibration to low $[Ti]_Q$. In the absence of any obvious mechanism, the authors assigned this to a fluid-mediated process, both in terms of enhancing Ti loss from within large quartz grains and transporting Ti through the intragranular medium. Therefore, ongoing research does indicate that the TitaniQ method can potentially be used at low temperatures in, for example, dynamically recrystallized rocks, as long as mechanisms for resetting $[Ti]_Q$ are fully constrained and understood. Results here suggest that even under fluid-absent or fluid-poor conditions, intragranular regions can act as the fast conduits for Ti migration/removal needed to explain Ti loss in dynamically metamorphosed quartz-rich rocks. In fact, processes such as sub-grain rotation which result in marked reduction of grain size should significantly enhance Ti mobility through the coupled processes of grain size reduction (i.e. limitation of rate-controlling lattice diffusion) and the development of a greater volume fraction of fast grain-boundary pathways. We

might even extrapolate from data presented here, which demonstrates considerable difference between flux of Ti through the quartz lattice vs grain boundary region, that development of subgrain boundaries within larger quartz grains might well be expected to promote fast Ti loss from large quartz grains, as also proposed by Bestmann and Pennacchioni (2015). The limitation in resetting $[Ti]_Q$ in quartz must remain the sluggishness of LD of Ti into and out of larger quartz grains. The model developed here in Figures 3 and 4 accounts for coupled grain boundary diffusion and lattice diffusion but in a simplified, type B regime of (Harrison, 1961). As such, it can only be applied meaningfully to the resetting of Ti concentrations in fine-grain rocks or in the rims of coarser grained rocks. Observations here do, however, support the observation that Ti depleted rims in quartz grains, as noted by Bestmann and Pennacchioni (2015), are expected due to the inherently faster mobility of Ti in grain boundary regions.

A type B kinetic regime noted in experiments here results in Ti enrichment at grain boundaries in polycrystalline quartz (i.e. higher temperatures). Similarly, resetting to higher temperatures in metamorphic rocks might also lead to enrichment in the rims of quartz grains. Huang and Audetat (2012) argued that fast growth kinetics of quartz grains can result in trapping of thermodynamically unstable, high Ti contents. Although they argued that this might be driven by the thermodynamically higher stability of Ti in grain boundary regions compared to quartz intragrains, a similar effect might be noted during rapid quartz growth in quartz-rich rocks with Ti enriched rims due to rapid grain boundary flux. Any limit in the extent to which artificially high Ti concentrations might develop would then be partly dependent on growth rates of quartz compared to lattice diffusivity. Lanzillo et al. (2014) suggested, based on results of their molecular dynamic simulations and using the empirical approach mentioned in Watson (2004), that ‘growth entrapment’ of high Ti concentrations originating from grain boundary regions in quartz was, even in a ‘worst case scenario’, of minor importance. Their calculation was made using a lower estimate of Ti diffusivity in near-grain boundary regions based on lattice diffusion data of Cherniak et al. (2007). If grain

boundary diffusivity, as measured here, is comparably to near-surface diffusivity, as Lanzillo et al. (2014) suggest, present results indicate that Ti entrapment during quartz growth must be negligible. High Ti contents in natural quartz are instead more likely to indicate resetting of Ti at higher temperatures, in the absence of any other mechanism which results in increased Ti concentrations. Furthermore, even during grain growth, the efficiency of grain boundary diffusion as a transport mechanism should be apparent in near-surface zonation of Ti contents of quartz.

The efficiency of grain boundary diffusion as a local transport process in quartz-rich rocks also has implications for the interpretation of textures seen in metamorphic rocks. Grain boundary diffusion provides a mechanism for mobilizing Ti, and might conceivably also be important in mobilizing other high field strength elements in other systems. Rutile-enriched veins, and localized crystallization of rutile in quartz-rich veins are commonly noted in high pressure rocks, and these features are sometimes interpreted as evidence for high Ti solubility in subduction zone fluids (for example, Gao et al. 2007 and references therein). Grain boundary diffusion could, over geologically realistic timescales as shown in Figure 4, mobilise Ti over several centimeters to decimeters, providing an alternative to the common assumption that local rutile enrichment necessarily implies fluid transport. Furthermore, enrichment in Ti along grain boundaries in quartz-rich rocks could also enrich Ti, and possibly other elements, into regions from which they can then be readily scavenged by permeating fluids.

Finally, as noted above, application of the TitaniQ geothermobarometer requires either Ti-saturated conditions or some estimate of Ti activity. Ti activity is non-trivial to determine, and typically estimated/assumed from the proximity of quartz grains to Ti-rich phases. The important contribution which grain boundaries play in Ti flux suggests, however, that in fine-grained quartz-rich rocks quartz grains might be considered Ti-saturated if they are in contact with a fine-grained intergranular medium, even if Ti-rich phases such as rutile are not

immediately adjacent. For example, from Figure 4, characteristic diffusion distances of Ti in fine-grained quartz (<10μm) are of the order of 10cm at 800°C over 10^5 years. By contrast, in coarse-grained rocks (>1mm), characteristic diffusion distances are of a similar order to grain size, implying that quartz grains can only be considered to be Ti saturated if they are in contact with Ti-rich phases or if a free-melt or fluid phase can be demonstrated to have been present.

Acknowledgements

Work was funded by the Leverhulme Trust and the School of GeoSciences, University of Edinburgh. The authors would like to extend their thanks to Ian Butler for assistance with laboratory work and to Chris Hayward for guidance and help with EMP analysis. The authors also thank 3 reviewers whose comments and advice improved this manuscript considerably and Linda Kirstein for useful discussion during preparation of the manuscript.

487 **Tables**

488 Table 1. Experimental conditions used in Ti diffusion in polycrystalline quartz experiments at
489 1.0 GPa and results determined by (i) fitting a single diffusion law to all data points, and (ii)
490 modelling the contributions of both lattice and grain boundary diffusion using the method of
491 LeClaire (1963). Grain Boundary diffusivity is determined assuming a grain boundary width
492 of 0.75 nm, segregation factor s=1 and by modelling the contribution of lattice diffusivity (D_L)
493 using the data of Cherniak (2007) as discussed in the text.

494

Run no.	T(^{0}C)	Duration (mins)	Single diffusion law for all data points		LeClaire (63) fit of grain boundary diffusion	notes
			D (m^2/s)	C_0 (ppm)	D_{gb} (m^2/s)	
TiQ5	1400	1430	$3.9\pm0.2\times10^{-15}$	$2.5\pm0.1\times10^{3}$	$2.1\pm0.1\times10^{-13}$	
TiQ6	1400	1531	$5.2\pm0.7\times10^{-15}$	$2.06\pm0.09\times10^{3}$	$1.4\pm0.2\times10^{-13}$	
TiQ7	1200	2755	$8.9\pm0.5\times10^{-15}$	$1.12\pm0.03\times10^{3}$	$2.3\pm0.1\times10^{-14}$	
TiQ9	1000	5806	$3.8\pm0.3\times10^{-15}$	$2.11\pm0.08\times10^{3}$	$1.89\pm0.07\times10^{-15}$	
TiQ10	1000	4364	$4.0\pm0.2\times10^{-15}$	$2.5\pm0.1\times10^{3}$	$2.26\pm0.07\times10^{-15}$	
TiQ11	1000	5829	$1.5\pm0.3\times10^{-13}$	$2.0\pm0.2\times10^{3}$	$5\pm3\times10^{-14}$	Free fluid phase present

495

496

Figure captions

Figure 1a) Typical diffusion pattern (from TiQ9) showing concentration of Ti in quartz with distance from the capsule wall (Ti source). Symbols larger than error bars unless shown. Data are fitted to a single diffusion law (dashed line) as discussed in text. b) Plot highlights a change in trend of the data, with the first part of the data obeying a diffusion law consisted with slower lattice diffusion and most data fitting reasonably well to a straight line fit, consistent with grain boundary diffusion in a type B kinetic regime. Scatter in data at the end of profile is due to greater error in Ti measurement at low Ti contents close to the detection limit. This part of the data was not used for fitting.

Figure 2. Temperature dependence of grain boundary diffusion of Ti in quartz. Error bars smaller than plot symbols unless shown. Open symbol is water-saturated experiment and was not used for fitting data. Arrhenius parameters extracted from the plot are: activation energy 195±7 kJ/mol and pre-exponential factor 2.00±0.08 $x10^{-7}$ m^2/s.

Figure 3. Arrhenius plot showing the temperature dependence of modelled effective total diffusivity of T in polycrystalline quartz (anhydrous) as a function of grain size. Calculated diffusivities consider the effects of both grain boundary diffusion (assuming a lower limit imposed by a segregation factor of s=1 and data for each experiment performed in this study) and lattice diffusion using the data of Cherniak et al., (2007).

Figure 4. Grain size dependence of characteristic diffusion distances in Ti in polycrystalline quartz as a function of temperature, calculated from total effective diffusivities given in Figure 3. Characteristic diffusion distances are calculated for 2 model end-members: time=10^5 years and time=10^7 years (see text for details). Bold lines are distances calculated using a segregation factor, s=1 for grain sizes labelled in the figure. Dashed lines are corresponding

525 distances determined based on strong partitioning of Ti into grain boundaries, s=20, as
526 discussed in the text.
527
528 **References**
529
530 Ashley, K.T., Webb, L.E., Spear, F.S., Thomas, J.B. (2013) P-T-D histories from quartz: A
531 case study of the application of the TitaniQ thermobarometer to progressive fabric
532 development in metapelites. *Geochemistry Geophysics Geosystems* **14**, 3821-3843.
533
534 Ayers, J.C., Brenan, J.B., Watson, E.B., Wark, D.A. and Minarik, W.G. (1992) A new capsule
535 technique for hydrothermal experiments using the piston-cylinder apparatus. *American*
536 *Mineralogist* **11**, 1080-1086.
537
538 Barker, A.K., Coogan, L.A., Gillis, K.M., Hayman, N.W., Weis, D. (2010) Direct observation
539 of a fossil high-temperature, fault-hosted, hydrothermal upflow zone in crust formed at the
540 East Pacific Rise. *Geology* **38**, 379-382.
541
542 Bestmann, M. and Pennacchioni, G. (2015) Ti distribution in quartz across a heterogeneous
543 shear zone within a granodiorite: The effect of deformation mechanism and strain on Ti
544 resetting. *Lithos* **227**, 37-56.
545
546 Blundy, J. and Wood, B. (2003) Partitioning of trace elements between crystals and melts.
547 *Earth and Planetary Science Letters* 210, 383-397.
548

549 Bromiley, G.D., Keppler, H., McCammon, C., Bromiley, F. and Jacobsen, S. (2004)
550 Hydrogen solubility and speciation in natural, gem-quality Cr-diopside. *American*
551 *Mineralogist*. **89**, 941-949.
552
553 Bromiley, G.D. and Hilairet, N. (2005) Hydrogen and minor element incorporation in
554 synthetic rutile. *Mineralogical Magazine* **69** (3), 345-358.
555
556 Bromiley, G.D., Shiryaev, A.A. (2006) Neutron irradiation and post-irradition annealing of
557 rutile (TiO_{2-x}): effect in hydrogen incorporation and optical absorption. *Physics and Chemistry*
558 *of Minerals* **33**, 426-434.
559
560 Bromiley, G.D., Nestola, F., Redfern, S.A.T. and Zhang, M. (2010) Water incorporation in
561 synthetic and natural MgAl2O4 spinel. *Geochimica et Cosmochimica Acta* **74**, 705-718.
562
563 Cherniak, D.J., Watson, E.B. and Wark, D.A. (2007) Ti diffusion in quartz. *Chemical Geology*
564 **236**, 65-74.
565
566 Cole, J.W., Deering, C.D., Burt, R.M., Sewell, S., Shane, P.A.R. and Matthews, N.E. (2014)
567 Okataina Volcanic Centre, Taupo Volcanic Zone, New Zealand: A review of volcanism and
568 synchronous pluton development in an active, dominantly silicic caldera system. *Earth-*
569 *Science Reviews* **128**, 1-17.
570
571 Cohen, A.J. and Makar, L.N. (1985) Dynamic biaxial absorption spectra of Ti^{3+} and Fe^{2+} in a
572 natural rose quartz crystal. *Mineralogical Magazine* **49**, 709-715.
573
574 Demouchy, S. (2010a) Diffusion of hydrogen in olivine grain boundaries and implications for
575 the survival of water-rich zones in the Earth's mantle. *Earth and Planetary Science Letters*
576 **295**, 305-313.

577

578 Demouchy, S. (2010b) Hydrogen diffusion in spinel grain boundaries and consequences for
579 chemical homogenization in hydrous peridotite. *Contributions to Mineralogy and Petrology*
580 **160**, 887-898.

581

582 Dohmen, R and Milke, R (2010) Diffusion in polycrystalline materials: Grain boundaries,
583 mathematical models, and experimental data. In: *Diffusion in Minerals and Melts*, Reviews in
584 Mineralogy and Geochemistry **72**, 921-970.

585

586 Gao, J., John, T., Klemd and Xiong, X. (2007) Mobilization of Ti-Nb-Ta during subduction:
587 Evidence from rutile-bearing dehydration segregations and veins hosted in eclogite,
588 Tianshan, NW China. *Geochimica et Cosmochinica Acta* **71**: 4974-4996.

589

590 Girard, G. and Stix, J. (2010) Rapid extraction of discrete magma batches from a large
591 differentiating magma chamber: the Central Plateau Member rhyolites, Yellowstone Caldera,
592 Wyoming. *Contributions to Mineralogy and Petrology* **160**, 441-465.

593

594 Grujic, D., Stipp, M. and Wooden, J.L. (2011) Thermometry of quartz mylonites: Importance
595 of dynamic recrystallization on Ti-in-quartz reequilibration. *Geochemistry Geophysics*
596 *Geosystems* **12**, Q06012

597

598 Harrison, L.G. (1961) Influence of dislocations of diffusion kinetics in solids with particular
599 reference to alkali halides. *Transactions of the Faraday Society* **57**, 1191-&.

600

601 Hayden, L.A. and Watson, E.B. (2007) Rutile saturation in hydrous siliceous melts and its
602 bearing on Ti-thermometry of quartz and zircon. *Earth and Planetary Science Letters* **258**,
603 561-568.

604

605 Hayden, L.A. and Watson, E.B. (2008) Grain boundary mobility of carbon in Earth's mantle:
606 A possible carbon flux from the core. *Proceedings of the National Academy* **105**, 8537-8541.
607
608 Hiraga T., Anderson, I.M. and Kohlstedt, D.L. (2003) Chemistry of grain boundaries in
609 mantle rocks. *American Mineralogist* **88**, 1015-1019.
610
611 Hiraga T., Anderson, I.M. and Kohlstedt, D.L. (2004) Grain boundaries as reervoirs of
612 incompatible elements in the Earth's mantle. *Nature*, **427**, 699-703.
613 Huang, R.F. and Audetat, A. (2012) The titanium-in-quartz (TitaniQ) thermobarometer: A
614 critical examination and re-calibration. *Geochimica et Cosmochimica Acta* **84**, 75-89.
615
616 Kohn, M.J. and Northrup, C.J. (2009) Taking mylonites' temperatures. *Geology* **37**, 47-50.
617
618 Lanzillo, N.A., Watson, E.B., Thomas, J.B., Nayak, S.K. and Curioni, A. (2014). Near-surface
619 controls on the composition of growing crystals: Car-Parrinello molecular dynamics (CPMD)
620 simulations of Ti energetics and diffusion in alpha quartz. *Geochimica et Cosmochimica Acta*
621 **131**, 33-46.
622
623 Leclaire, A.D. (1963) Analysis of grain boundary diffusion measurements. *British Journal of*
624 *Applied Physics* **14**, 351.
625
626 Mehrer, H. (2007). D*iffusion in Solids: Fundamentals, Methods, Materials, Diffusion-*
627 *controlled Processes*. Springer, Berlin.
628
629 Müller, A., Herrington, R., Armstrong, R., Seltmann, R., Kirwin, D., Stenina, N. and Kronz, A.
630 (2010) Trace elements and cathodoluminescence of quartz in stockwork veins of Mongolian
631 porphyry-style deposits. *Mineralium Deposita* **45**, 707-727.
632

633 Negrini, M., Stunitz, H., Berger, A. and Morales, L.F.G. (2014). The effect of deformation on
634 the TitaniQ geothermobarometer: an experimental study. *Contributions to Mineralogy and*
635 *Petrology* **167**, 982.
636
637 Nogueira, M.A.d.N., Ferraz, W.B. and Sabioni, A.C.S. (2003) Diffusion of the ^{65}Zn radiotracer
638 in ZnO polycrystalline ceramics. *Materials Research* **6**, 167-171.
639 Pennacchioni, G., Menegon, L., Leiss, B., Nestola, F. and Bromiley, G. (2010) Development
640 of crystallographic preferred orientation and microstructure during plastic deformation of
641 natural coarse-grained quartz veins. *Journal of Geophysical Research-Solid Earth* **115**
642 B12405.
643
644 Rusk, B.G., Lowers, H.A. and Reed, M.H. (2008) Trace elements in hydrothermal quartz:
645 Relationships to cathodoluminescent textures and insights into vein formation. *Geology* **36**,
646 547-550.
647
648 Sato, K. and Santosh, M. (2007) Titanium in quartz as a record of ultrahigh-temperature
649 metamorphism: the granulites of Karur, southern India. *Mineralogical Magazine* **71**, 143-154.
650
651 Spear, F.S. and Wark, D.A. (2009) Cathodoluminescence imaging and titanium thermometry
652 in metamorphic quartz. Journal of Metamorphic *Geology* **27**, 187-205.
653
654 Storm, L.C. and Spear, F.S. (2009) Application of the titanium-in-quartz thermometer to
655 pelitic migmatites from the Adirondack Highlands, New York. *Journal of Metamorphic*
656 *Geology* **27**, 479-494.
657
658 Sutton, A.P. and Balluffi, R.W. (1995) *Interfaces in Crystalline Materials*. Oxford Science
659 Publications, Oxford.
660

661 Thomas, J.B., Watson, E.B., Spear, F.S., Shemella, P.T., Nayak, S.K. and Lanzirotti, A.
662 (2010) TitaniQ under pressure: the effect of pressure and temperature on the solubility of Ti
663 in quartz. *Contributions to Mineralogy and Petrology* **160**, 743-759.
664
665 Vazquez, J.A., Kyriazis, S.F., Reid, M.R., Sehler, R.C. and Ramos, F.C. (2009)
666 Thermochemical evolution of young rhyolites at Yellowstone: Evidence for a cooling but
667 periodically replenished postcaldera magma reservoir. *Journal of Volcanology and*
668 *Geothermal Research* **188**, 186-196.
669
670 Wark, D.A., Hildreth, W., Spear, F.S., Cherniak, D.J. and Watson, E.B. (2007) Pre-eruption
671 recharge of the Bishop magma system. *Geology* **35**, 235-238.
672
673 Wark, D.A. and Watson, E.B. (2006) TitaniQ: a titanium-in-quartz geothermometer.
674 *Contributions to Mineralogy and Petrology* **152**, 743-754.
675
676 Watson, E.B. (2004) A conceptual model for near-surface kinetic controls on the trace-
677 element and stable isotope composition of abiogenic calcite crystals. *Geochimica et*
678 *Cosmochimica Acta* **68**, 1473-1488.
679
680 Whipple, R.T.P. (1954) Concentration contours in grain boundary diffusion. *Philosophical*
681 *Magazine* **45**, 1225-1236.
682
683 Wu, J. and Koga, K.T. (2013) Fluorine partitioning between hydrous minerals and aqueous
684 fluid at 1 GPa and 770-947 °C: A new constraint on slab flux. *Geochimica et Cosmochimica*
685 *Acta* **119**, 77-92.
686

687 Figure 1

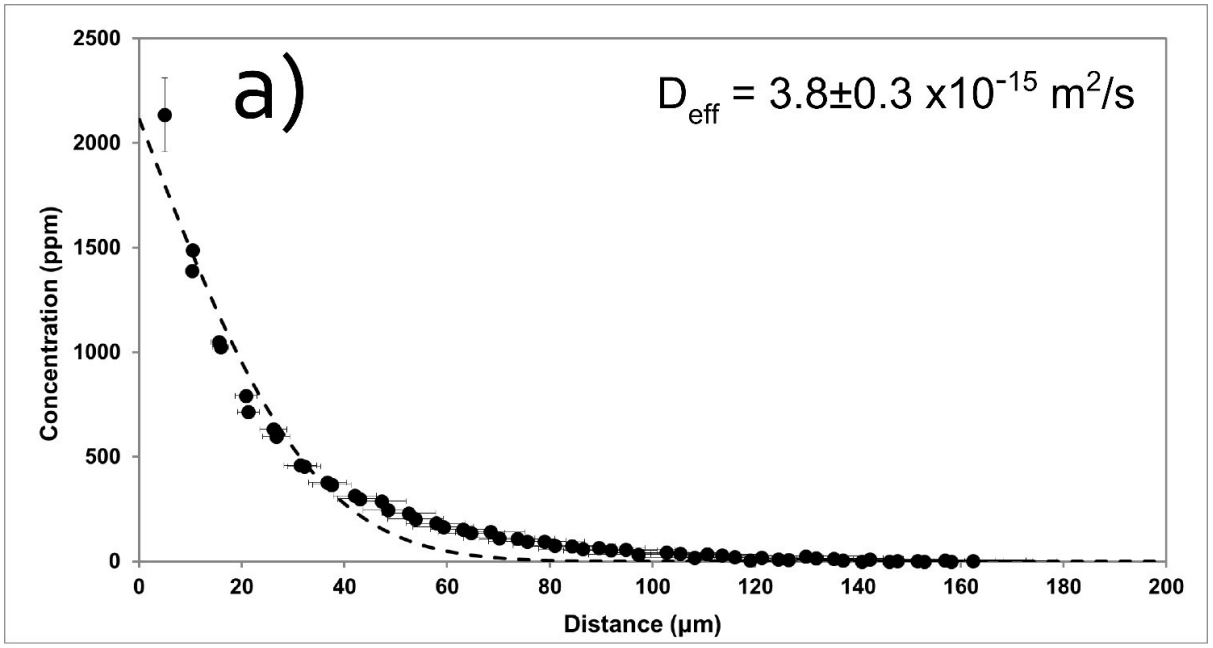

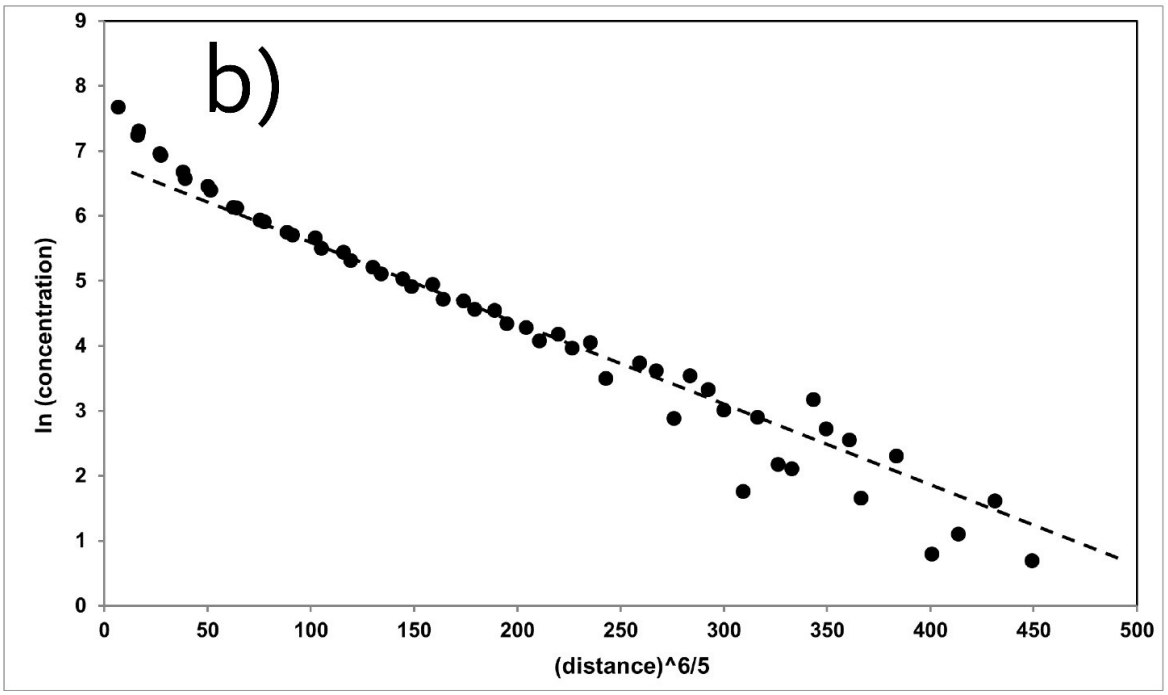

688

689

690 Figure 2

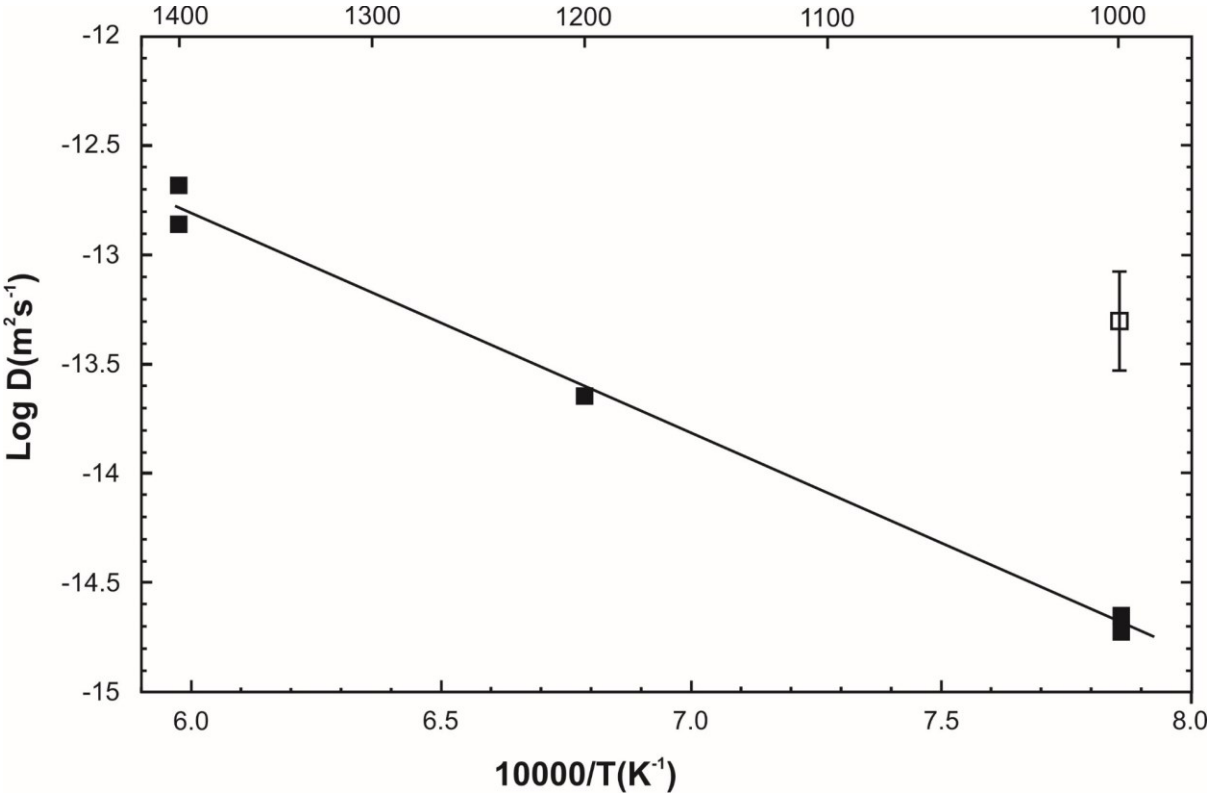

691

692

693 Figure 3

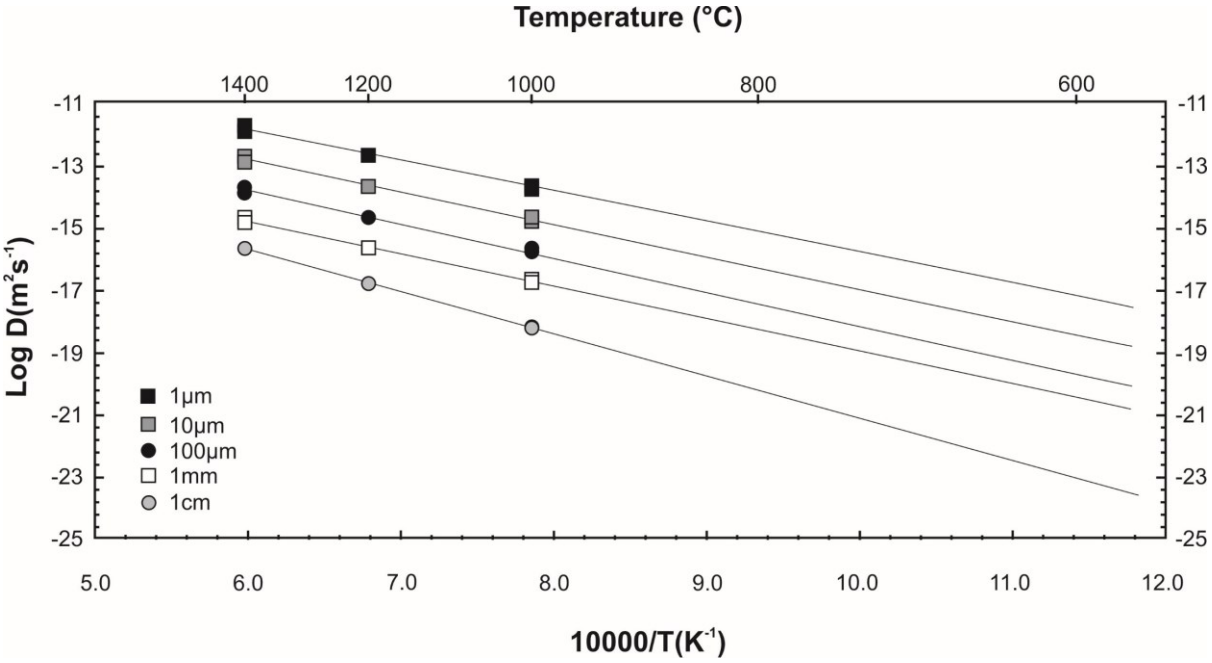

694

695

696 Figure 4

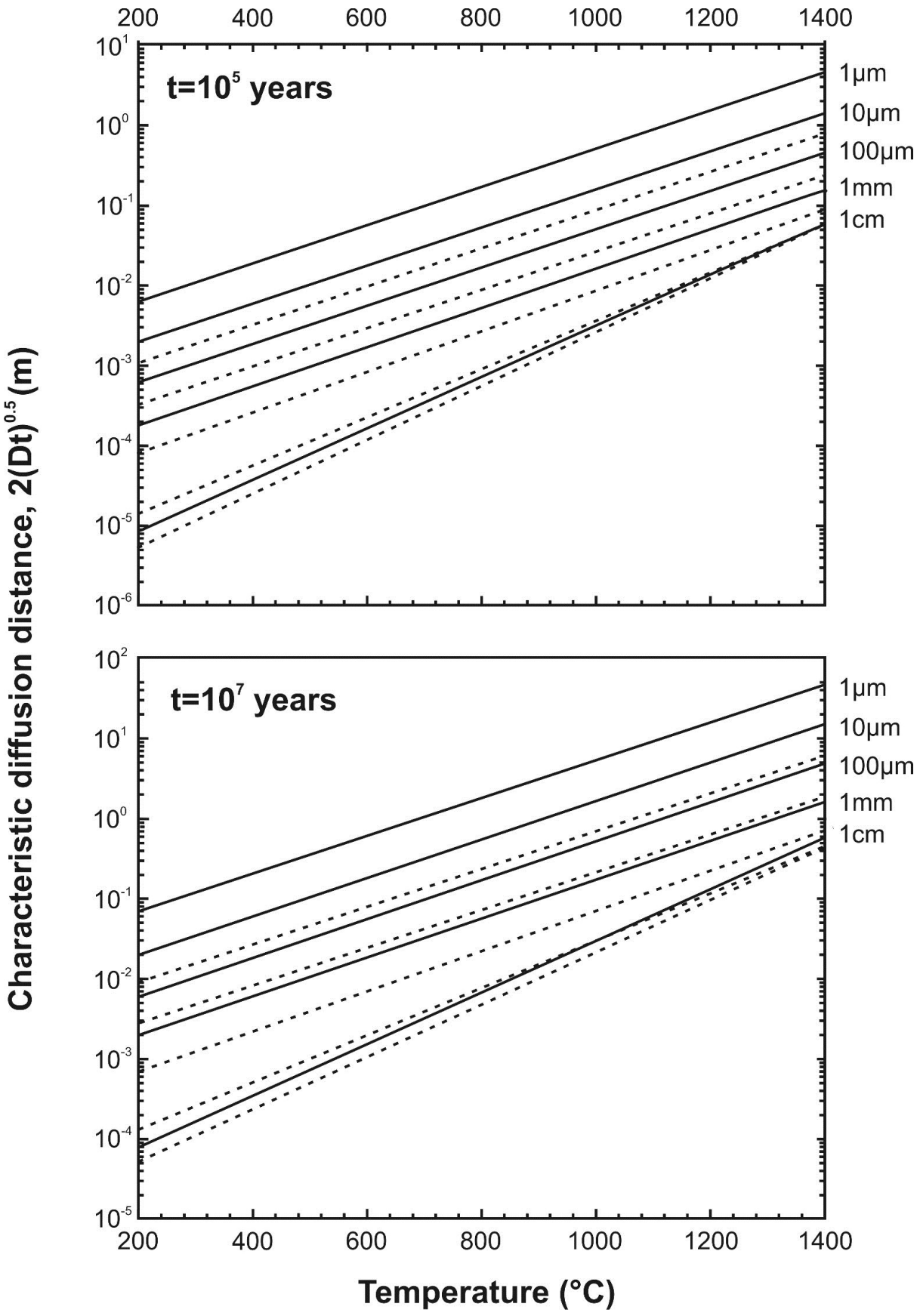

697

698